Open access • Journal Article • DOI:10.1038/NCB1782

The ABC transporter AtABCB14 is a malate importer and modulates stomatal response to CO2. — Source link

Miyoung Lee, Yongwook Choi, Bo Burla, Bo Burla ...+7 more authors

Institutions: Pohang University of Science and Technology, University of Zurich, Nagoya University

Published on: 07 Sep 2008 - Nature Cell Biology (Nature Publishing Group)

Topics: Malate transport, Guard cell, Apoplast and Light intensity

The ABC transporter AtABCB14 is a malate importer and modulates stomatal response to CO2

Lee, M; Choi, Y; Burla, B; Kim, Y Y; Jeon, B; Maeshima, M; Yoo, J Y; Martinoia, E; Lee, Y

The ABC transporter AtABCB14 is a malate importer and modulates stomatal response to CO2

Abstract

Carbon dioxide uptake and water vapour release in plants occur through stomata, which are formed by guard cells. These cells respond to light intensity, CO2 and water availability, and plant hormones. The predicted increase in the atmospheric concentration of CO2 is expected to have a profound effect on our ecosystem. However, many aspects of CO2-dependent stomatal movements are still not understood. Here we show that the ABC transporter AtABCB14 modulates stomatal closure on transition to elevated CO2. Stomatal closure induced by high CO2 levels was accelerated in plants lacking AtABCB14. Apoplastic malate has been suggested to be one of the factors mediating the stomatal response to CO2 (Refs 4,5) and indeed, exogenously applied malate induced a similar AtABCB14-dependent response as high CO2 levels. In isolated epidermal strips that contained only guard cells, malate-dependent stomatal closure was faster in plants lacking the AtABCB14 and slower in AtABCB14-overexpressing plants, than in wild-type plants, indicating that AtABCB14 catalyses the transport of malate from the apoplast into guard cells. Indeed, when AtABCB14 was heterologously expressed in Escherichia coli and HeLa cells, increases in malate transport activity were observed. We therefore suggest that AtABCB14 modulates stomatal movement by transporting malate from the apoplast into guard cells, thereby increasing their osmotic pressure.

The ABC transporter AtABCB14 is a malate importer and modulates stomatal response to CO_2

Miyoung Lee[a,b], Yongwook Choi[b], Bo Burla[a,c], Yu-Young Kim[a,b], Byeongwook Jeon[a,b], Masayoshi Maeshima[d], Joo-Yeon Yoo[b], Enrico Martinoia[1,a,b,c] and Youngsook Lee[1,a,b]

[a] Postech-UZH Global Research Laboratory and [b]Department of Life Science, Pohang University of Science and Technology, Pohang, 790-784, Korea; [c]Institute of Plant Biology, University of Zurich, Zollikerstrasse 107, 8008 Zürich, Switzerland; and [d]Laboratory of Cell Dynamics, Graduate School of Bio agricultural Sciences, Nagoya University, Nagoya, 464-8601 Japan

[1]These authors contributed equally to the manuscript.

Carbon dioxide uptake and water vapour release of plants occur through stomata that are formed by the guard cells, which respond to light intensity, CO_2, H_2O availability and plant hormones[1,2]. The predicted increase of atmospheric [CO_2] is expected to have a profound impact on our ecosystem, however, many aspects of CO_2-dependent stomatal movements are still not understood[3]. Here we show that the ABC transporter AtABCB14 modulates the stomatal closure upon transition to elevated [CO_2]. High [CO_2] induced stomatal closure was accelerated in plants lacking AtABCB14. Apoplastic malate has been suggested to be one of the factors mediating stomatal response to [CO_2][4,5] and indeed exogenously applied malate induced a similar AtABCB14-dependent response as high [CO_2]. In isolated epidermal strips which contained only guard cells, malate-dependent stomatal closure was faster from plants lacking the AtABCB14, and slower in AtABCB14 over-expressing plants, than in wild type, indicating that AtABCB14 catalyzes the transport of malate from the apoplast into guard cells. Indeed, when AtABCB14 was heterologously expressed in *E. coli* and HeLa cells, increases in malate

transport activity were observed. We therefore suggest that AtABCB14 modulates stomatal movement by transporting malate from the apoplast into guard cells, thereby increasing their osmotic pressure.

The ABC transporter family is one of the largest gene families. Members of this family are present in all taxa and have a very broad range of functions[6]. Plant ABC transporters are implicated in tasks as diverse as cellular detoxification of organic toxins and heavy metals, resistance against pathogens, transport of long chain fatty acids and of phytohormones, and regulation of the stomatal aperture[7,8]. In our attempts to elucidate physiological roles of hitherto undescribed ABC transporters, we noted that *AtABCB14*[9] *(also known as AtPGP14*[7] *or AtMDR12*[8]*)* was strongly expressed in guard cells. Other ABC transporters, i.e. AtMRP4 and AtMRP5, have recently been identified as components of the complex regulatory network of guard cell movement. An AtMRP5 knock-out mutant was impaired in anion channel regulation[10-12] and had a strongly reduced sensitivity to glibenclamide, ABA, calcium and auxin, which are well known to control stomatal movement. We therefore were interested whether AtABCB14 also exhibits a regulatory function in guard cell physiology.

AtABCB14 expression, as visualized by the activity of an *AtABCB14 promoter::GUS* fusion construct, is not restricted to guard cells of leaves only, but is also found in guard cells of stems, flowers and siliques (Fig. 1a-f). In leaves, GUS activity was also detected in epidermal and at very low levels in mesophyll cells (Fig. 1c). These promoter::GUS expressions corresponded to the transcript levels detected in mesophyll and guard cell protoplasts (Fig. 1g). Transient expression of an *35S::AtABCB14:GFP* construct in *Arabidopsis* protoplasts revealed that AtABCB14 is targeted to the plasma membrane (Fig. 1h, i). *AtABCB14:sGFP* expressed under the control of the *AtABCB14* native promoter was targeted to the plasma membrane of guard cells (Fig. 1n). Coexpression of AtABCB14 with AtAHA2:RFP, a fusion protein

of a plasma membrane localized proton pump with a red fluorescent protein[13], resulted in a perfect co-localization (Fig. 1j- l). Fractionation of microsomes on a sucrose density gradient further confirmed that AtABCB14:HA protein was targeted to the plasma membrane: the distribution pattern of the protein crossreacting with the HA antibody corresponded to that of AtPDR8, a plasma membrane protein[14] and differed from the patterns of the ER (Bip) and vacuolar markers (γ–TIP) (Fig. 1m). These results indicate that AtABCB14 is a plasma membrane localized protein.

We obtained two allelic *AtABCB14* T-DNA insertion mutants (SALK_016005 and SALK_026876, designated *atabcb14-1* and *atabcb14-2*, respectively) and identified homozygous knockout plants with no detectable *AtABCB14* transcripts (see Supplementary Information, Fig. S2a, b). In addition, we generated plants in which *AtABCB14* expression was driven by the CaMV-35S promoter, and identified plants with increased *AtABCB14* transcript levels in guard cells as well as in whole plants (see Supplementary Information, Fig. S2b). Stomatal apertures of mutant plants did not significantly differ from those of wild-type plants under illumination or darkness (data not shown). To elucidate whether AtABCB14 is implicated in one of the other known guard cell signal transduction pathways[2,15-17], we assayed stomatal apertures in response to ABA and Ca^{2+}. In neither case did we observe a behaviour different from that of the wild-type plants (see Supplementary Information, Fig. S2c, d). Stomatal aperture is also regulated by the $[CO_2]$. Stomata open at low $[CO_2]$ and close in response to elevated $[CO_2]$[18]. Interestingly, after exposure to elevated $[CO_2]$, stomatal closure was more pronounced in *atabcb14* deletion mutants, whereas it was reduced in mutants overexpressing AtABCB14, compared to wild-type plants (Fig. 2a). Stomatal apertures of 3 independent complemented *AtABCB14* knockout lines were similar to that of wild-type plants under elevated $[CO_2]$ (see Supplementary Information, Fig. S3b). The differential stomatal response of the genotypes was also confirmed by gas exchange analysis (Fig. 2b). Initial rates in decrease of stomatal conductance after raising $[CO_2]$

from 100 to 800 ppm were higher for the mutants *atabcb14-1* and *2* (0.067 and 0.062 relative conductance units per minute) than for wild-type plants (0.040).

Recent evidence suggests that CO_2 can be perceived directly by guard cells[19,20]. However, previous studies supported an additional scenario in which apoplastic malate released from mesophyll cells in response to elevated [CO_2] mediates the effect of [CO_2] on stomata by shifting the current-voltage curve of anion channels towards resting membrane potentials, and thereby increasing the probability of opening of the anion channels[4,5,21,22]. Anion channel opening results in the release of anions from guard cells and in subsequent stomatal closure[23,24]. However, once malate has been taken up into guard cells, it acts as an osmoticum and induces guard cell swelling. When *Arabidopsis* leaves were floated on 20 mM malate at pH 6.15, stomatal closure of wild-type and mutant plants was consistently reduced compared to leaves kept under elevated [CO_2], but the pattern of differences between the different *AtABCB14* genotypes was similar to that observed under elevated [CO_2] (Fig. 2c and see Supplementary Information, Fig. S3c). Similar, but less pronounced differences were observed using 5 mM malate (see Supplementary Information, Fig. S4a). These results suggest that AtABCB14 is involved in the CO_2-dependent regulation of stomatal movement and that part of the CO_2 response is mediated by malate.

To dissect the mechanism of the AtABCB14-dependent response of stomata to CO_2 and malate, we first tested whether guard cells in epidermal strips also show differential responses similar to whole leaves. For this purpose, we isolated epidermal strips where the epidermal cells were disrupted containing viable guard cells only. The absence of neighbour cells, which normally exhibit a strong counter pressure on the guard cells, reduced the extent of the stomatal aperture changes under this condition. Under light conditions, exposure of the epidermal strips to high [CO_2] resulted in a decrease of stomatal aperture (CO_2 in Fig. 2d and see Supplementary Information, Fig.

S4b), supporting the previously mentioned scenario that of a guard cell-autonomous perception and response to elevated [CO_2][19,20]. However, no difference in the responses was observed between wild-type plants, deletion mutants and AtABCB14 overexpressing plants. In contrast, when epidermal strips were exposed to malate, striking differences were observed between the genotypes. Compared to wild-type plants, deletion mutants closed their stomata more tightly, while AtABCB14 overexpressing plants did not close their stomata at all (MA in Fig. 2d and see Supplementary Information Fig. S4b). These differences between the genotypes were similar to that found in whole leaves under elevated [CO_2] (Fig. 2a), and thus suggest that the function of AtABCB14 during stomatal closing under high [CO_2] depends on the presence of apoplastic malate. Apoplastic malate concentrations have been reported to increase from 1 to more than 3 mM in response to an increase in the CO_2 level from ambient to 672 ppm[5]. The opposite phenotype to that observed in our study was recently described for the SLAC1 mutants[25,26]. In SLAC1 deletion mutants the activity of the slow anion channel is impaired. Consequently, efflux of anions is strongly reduced and stomata close only partially. Since in our case the absence of AtABCB14 induces a faster stomata closure, a malate importer at the plasma membrane of guard cells could explain our observations. In the absence of a malate importer, malate cannot be taken up and decrease the osmotic pressure within the guard cells, but acts only on the anion channel, inducing rapid stomatal closure. In wild-type and overexpressing plants, malate is taken up into guard cells and exhibits a major role as an osmoticum, inducing stomatal opening. A further support for the role of AtABCB14 as a malate importer was obtained from an experiment in which opening of closed stomata was tested. When malate was the sole anion in the bathing medium, stomata opened quicker in AtABCB14 overexpressing plants, while they opened more slowly in the two *atabcb14* mutants (Fig. 2e). Such a transport may be important under high [CO_2], and is also likely to play a role in recycling apoplastic malate under normal [CO_2]. It is interesting

to note that in medium without malate, stomata of *AtABCB14* mutants did not differ from wild type in light-induced opening (data not shown). Since under light, photosynthesis decreases leaf internal [CO_2], and malate levels in the apoplast remain very probably low under ambient [CO_2], it is not surprising that mutations in a malate importer gene do not alter stomatal responses to light.

In order to elucidate whether the observed phenotype is indeed due to an AtABCB14 mediated malate transport activity, we heterologously expressed AtABCB14 in the dicarboxylate transporter mutant CBT315 of *E. coli* which cannot utilize malate as a carbon source. Wild type *E. coli* grew well, while CBT315 containing the empty vector (CBT315-EV) did not grow at all on malate containing medium. Complementation of CBT315 with AtABCB14 (CBT315-A14) partially restored growth of CBT315 (Fig. 3a). ^{14}C-malate uptake was low in CBT315-EV and high in CBT315-A14, showing that expression of AtABCB14 strongly increased malate uptake (Fig. 3b). Inhibitors used to characterize ABC transporters, such as vanadate, verapamil and cyclosporin A, inhibited malate transport activity[6, 27,28] (Fig. 3c). Despite the fact that these inhibitors are not specific for ABC transporters only[6], the consistent partial inhibition observed with these different inhibitor classes strongly indicate that an ABC-type transporter is involved in AtABCB14-mediated malate uptake. Incomplete inhibition by these agents may be explained by either a slow loading of the inhibitors or their efficient extrusion from the cells. Yet, the inhibition *per se* strongly supports that malate uptake is mediated by the transport activity of AtABCB14. In line with these results is the observation that uptake of ^{14}C-malate is strongly inhibited by unlabeled malate and fumarate but not by nitrate or chloride (Fig. 3d), excluding the possibility that the malate uptake is just a result of increased permeability. Citrate and succinate compete only weakly. Fumarate, which is present in high concentrations in *Arabidopsis* leaves[29] acts like malate in closing stomata (see Supplementary Information, Fig. S4c). To additionally test malate transport activity in an eukaryotic expression system, we

used HeLa cells. Our results show that HeLa cells expressing the empty vector exhibit an intrinsic malate uptake activity. However, expression of AtABCB14 increased malate transport by 80%, demonstrating that AtABCB14 exhibits malate uptake activity also in HeLa cells (Fig. 3e). The observation that malate uptake was increased in both *E. coli* and HeLa cells expressing AtABCB14 strongly supports our hypothesis that AtABCB14 is a malate importer.

Under our standard growth conditions, flowering times of deletion mutants and wild type were similar, but that of AtABCB14 overexpressing plants was consistently later than that of deletion mutants (Fig. 4a, c and see Supplementary Information, Fig. S5a, b). A similar difference in flowering time was observed when plants were either subjected to high [CO_2] (data not shown) or drought conditions (see Supplementary Information, Fig. S5c, d). However, when plants were simultaneously exposed to elevated [CO_2] and drought, the difference in floral induction became very pronounced: overexpressing plants (*35S::A14-1*) opened their first flowers eleven days later than deletion mutants (*atabcb14-1*) (Fig. 4b, c and see Supplementary Information, Fig. S5a, b). These results are consistent with the observation that stress symptoms are usually accentuated under high [CO_2][18]. Additionally, the number of rosette leaves at the time of flowering was determined. Under normal conditions, numbers were similar between mutant and wild-type plants, however under the combined high [CO_2] and drought condition, leaf numbers at the time of flowering were higher in overexpressing plants and lower in knockout plants compared to wild-type plants (Fig. 4d and see Supplementary Information, Fig. S5b). These results indicate that AtABCB14 affects floral induction under the combination of high [CO_2] and drought. The difference in flowering time of *AtABCB14* mutant plants demonstrates that AtABCB14 mediated malate uptake across the plasma membrane has a major impact on plant growth under stress condition.

In this paper, we present strong evidence that the ABC transporter AtABCB14 is a malate import protein. This is a surprising finding, since so far, no plasma membrane localized ABC transporter has been shown to transport any primary metabolite. AtABCB14 is highly expressed in guard cells and our results suggest that AtABCB14 mediates malate accumulation within the guard cells which acts as an osmoticum and induces guard cell swelling. Such an uptake mechanism allows to recycle malate and possibly fumarate released in response to high [CO_2] or during normal stomatal closure. Our observations that the malate transporter AtABCB14 modulates the stomatal responses to elevated [CO_2] supports the previously proposed hypothesis that apoplastic malate is an important element in guard cell regulation. It remains to be determined which cell types are the major source of apoplastic malate during the response to high [CO_2], since both guard cells and mesophyll cells have been reported to release malate into apoplast[4,5,30]. Our results support the hypothesis that CO_2 acts on two independent pathways that both modulate guard cell movement. One is directly mediated by CO_2, and the other is indirectly mediated by malate secreted into the apoplast in response to elevated [CO_2]. Interestingly, *AtABCB14* transcript levels are not significantly altered under high [CO_2] in the presence of malate (data not shown). This may indicate that modulation of AtABCB14 activity occurs by secondary modifications, which allows a rapid adjustment in response to environmental changes. The elucidation of the factors modifying AtABCB14 activity will be a fascinating future work.

Methods

Plant material and growth conditions. All *Arabidopsis* wild-type plants used in this study were of the *Columbia-0* ecotype. Plants were grown on soil under 16/8 h cycles of light (40 µmol $m^{-2}s^{-1}$) at 22˚C and dark at 18˚C.

Verification of *AtABCB14 k*nockout and over-expressing *Arabidopsis* plants. Two independent T-DNA insertion lines in the *AtABCB14* were obtained from the Salk Institute Genomic Analysis Laboratory (http://signal.salk.edu/cgi-bin/tdnaexpress) and designated as *atabcb14-1* (SALK_016005) and *atabcb14-2* (SALK_026876). Homozygote *AtABCB14* knockout plants were selected by PCR using the genomic DNA as the template. To confirm the T-DNA insertion in the *AtABCB14* gene, we used the T-DNA specific primer 5'-GCGTGGACCGCTTGC TGCAACT-3' and the *AtABCB14* specific primer 5'-TGGTCAAGTTAGGGAAACCGGA-3'. To select homozygous lines of *atabcb14-1* and *atabcb14-2*, we performed PCR using the primers 5'-AAGCTCGTCCTCAATGATATGGG-3' and 5'-GCCCATCGATACAGAGATT TCCG-3' for the *atabcb14-1* line, and 5'-ACTTGTGAACTAAGCAAACCCACCA-3' and 5'-GTCTTTTTGTCCCACCCAAGAGTTC-3' for the *atabcb14-2* line. The abundance of the *AtABCB14* transcript in homozygous lines of *atabcb14-1*, *atabcb14-2*, *35S::A14-1, 35S::A14-2*, and wild type plants was assayed by RT-PCR. Total RNA was extracted from whole seedlings and RT-PCR was performed using primers specific for *AtABCB14*: 5'-GAGACTGAAA TACCTCCAGACCAGC-3', 5'-GCTCGTCCTCAATGATATGGGAACT-3' and 5'-TCTAGATCACACCGCT TCTTGAAGACTCGTCAATTT-3'. As a loading control *Tubulin1* transcript was amplified with the primers 5'-CTCACAGTCCCGGA GCTGACAC-3' and 5'-GCTTCAGTGAACTCCATCTCGT-3'.

DNA constructs. Full-length cDNA of *AtABCB14* was amplified from cDNA generated from total RNA extracted from wild type seedlings by PCR using primers containing *BamH*I restriction sites (5'-GTCGACGGATCCATGGATAACATAGAACCACCCT TTAGTGG-3' and 5'-GGATCCCTCGAGTCACACCGCTTCTTGAAGACTCGTCAA TTT-3'). This fragment was then subcloned into the pGEM-T easy vector (Promega, Madison, WI). For subcellular localization studies, a *BamH*I fragment of this construct was ligated into the transient expression vector 326-sGFP (Clontech, CA). The

construct to generate AtABCB14 overexpressing plants was created by ligating the *BamH*I fragment of the *AtABCB14* cDNA construct into pBI121. The *AtABCB14 Promoter*::GUS reporter gene construct was made by PCR amplification of a 2 kb promoter region of *AtABCB14* from genomic DNA using primers containing *BamH*I restriction sites (5'-GGATCCGAATTCCTTAAACTTAATGAAAATGGATG GGAATTGATGCGTA-3' and 5'-CTGCAGCCATGGGGATCCTATCACTTTAGC ACTGTGACT TACTAAAACAGA-3'), and ligation of the fragment into pBI101.1. To generate complemented lines of *atabcb14-1* mutants, the *AtABCB14* promoter was inserted into pCAMBIA1302 (BIOS, CA) using *EcoR*I and *Pst*I, and the *BamH*I fragment of the subcloned *AtABCB14* cDNA was ligated into the same vector using *BamH*I site, which was introduced by the insertion of the promoter fragment. HA tag amplified from pHB-HA3 (ABRC stock number: CD3-591) was fused to the 3'-end of *AtABCB14.* This construct was further modified to generate transgenic *Arabidopsis* expressing *AtABCB14:sGFP* under the *AtABCB14* native promoter. The HA tag was replaced by sGFP amplified by PCR with a pair of primers containing a *Mlu*I restriction site (5'-TTTACGCGTGGTCACCTTACTTGTACAGCTCGTCCA-3' and 5'-ACGAGAACGCGTCAGAGGCA-3'). All constructs were verified by sequencing.

RT-PCR of mesophyll and guard cell protoplasts. Mesophyll or guard cell protoplasts were isolated from 4-5 week-old leaves following the method of Abel & Theologis[31] or Hwang *et al*.[32], respectively. Released guard cell protoplasts were collected using a patch-clamp glass pipette. Total RNA was extracted from the collected cells using a Picopure RNA isolation kit (Arcturus, Mountain View, CA)[33], and used for detection of *AtABCB14* transcript by RT-PCR . Band intensities were quantified using Photoshop CS3 Extended (Adobe Inc, CA, USA).

Isolation, fractionation and immunoblotting of microsomes. Fractionation using sucrose density gradient was performed according to Kobae *et al*.[14] with some

modifications. Plants were homogenized in homogenizing solution (50 mM Tris–HCl, pH 8.0, 250 mM sorbitol, 10 mM EDTA, 4 mM dithiothreitol, 0.1% 2-mercaptoethanol and 100 μM *p*-(amidinophenyl) methanesulfonyl fluoride hydrochloride). The homogenate was filtered through 200 μm mesh and centrifuged at 10,000×*g* for 10 min. The supernatant was centrifuged at 100,000×*g* for 1 h and the resulting microsomal pellet was resuspended in the homogenizing solution, loaded onto sucrose gradient (15-45% (w/w)), and centrifuged at 77,000×*g* for 17 h. After centrifugation, 27 fractions were collected and used for immunoblotting.

Stomatal aperture and gas exchange measurements. Stomatal apertures were assayed from 5 week-old leaves. Detached whole leaves were incubated on 10 mM MES-KOH and 0.1 mM $CaCl_2$ buffer containing either 5 or 20 mM malate (L-malic acid, disodium salt) or 10 mM KCl. Final pH of all buffers was set to 6.15. Stomatal conductance of wild type, *atabcb14-1* and *2* were measured using the LI-COR LI-6400 (LI-COR Inc, NE, USA), with a LI-6400-40 light source set to 150 μmol s^{-1} m^{-2} quanta with 10% blue light. Relative humidity of incoming air was maintained at 67% ± 5.

Heterologous expression of AtABCB14 in *E. coli*, complementation and transport assays. The dicarboxylate transport (*dct*) mutant CBT315 (CGSC#:5269) and its isogenic wild type, K12 (CGSC#:4401) were obtained from the *E. coli* Genetic Resources Center of Yale University (http://cgsc.biology.yale.edu). ^{14}C-malate uptake was assayed according to Jeong *et al.*[34] with minor modifications. *AtABCB14* was inserted into the *EcoR*I site of pKK223-3. For functional complementation tests, *E. coli* transformed with empty vector or *AtABCB14* were grown on M9 medium containing 10 mM L-malic acid (pH adjusted to 6.6 with NaOH) at 37˚C for 4 days.

For malate transport assays, strains were cultured in LB medium and harvested at mid-log phase. Cells were washed twice using 50 mM potassium phosphate buffer (pH 5.9), and resuspended in the same buffer at an OD_{600}=10. Malate uptake was initiated by

adding 1 mM L-^{14}C malic acid (Amersham Biosciences) with a specific activity of 4.5 kBq µmol^{-1} to the cell suspension. After the indicated incubation period in the graph, the suspensions were filtered through nitrocellulose membranes and the cells washed with 500 µl of ice-cold 0.1 M LiCl. The radioactivity on the filters was determined by liquid scintillation counting.

Transport assay using HeLa cells. For transient expression of AtABCB14 in HeLa cells, cDNA of *AtABCB14* was ligated into the *EcoR*I site in pCDNA3 vector (Invitrogen, Carlsbad, CA). To introduce the plasmid DNA into the cells, HeLa cells were detached by trypsin and mixed with 2 µg DNA of pCDNA3 or pCDNA3-*AtABCB14* and metafectene pro (Biontex, Munich, Germany). The same numbers of cells ($3*10^5$) were aliquoted into six-well plates. After 30 hours of incubation, cell numbers were counted again to check that the cell numbers of experimental samples were similar. The transport assays in HeLa cell were performed as described in Geisler *et al.*[27] and Kimoto *et al.*[35] with some modifications. Cells were washed with 1 ml of pre-warmed Dulbecco's modified Eagle's medium containing 5% fetal bovine serum and incubated in 0.6 ml of pre-warmed HBSS-MES buffer (25 mM D-glucose, 137 mM NaCl, 5.37 mM KCl, 0.3 mM Na_2HPO_4, 0.44 mM KH_2PO_4, 1.26 mM $CaCl_2$, 0.8 mM $MgSO_4$, 10 mM MES, pH 5.8) including 5% fetal bovine serum for 10 minutes. The uptake assay was started by adding ^{14}C-malic acid (specific activity of 6.02 KBq µmol^{-1}). After 10 minutes of incubation at 37°C and 5% CO_2, cells were washed three times with 2.3 ml of ice-cold HBSS-MES buffer, and detached from the well plate by treatment with trypsin. Detached cells were transferred into the scintillation cocktail solution and radioactivity was counted. For the 0 min time point, cells were directly washed as described above after the addition of radiolabelled malate. To check *AtABCB14* expression, RT-PCR was performed using total RNA extracted from pCDNA3 or pCDNA3-*AtABCB14* expressing HeLa cells. *β-actin S*: 5'-

TCTACAATGAGCTGCGTGTG-3' and *β-actin AS*: 5'-ATCTCCTTCTG CATCCTGTC-3' were used as primers for the loading control.

Accession numbers. The Genbank accession number of *AtABCB14* is NM_102566, and the AGI number is At1g28010.

1. Fan, L., Zhao, Z. & Assmann, S.M. Guard cells: a dynamic signaling model. *Curr. Opin. Plant Biol.* **7,** 537-546 (2004).

2. Hetherington, A.M. Guard cell signaling. *Cell* **107,** 711-714 (2001).

3. Schroeder, J.I. *et al*. Guard cell ABA and CO_2 signaling network updates and Ca^{2+} sensor priming hypothesis. *Curr. Opin. Plant Biol.* **9,** 654-663 (2006).

4. Hedrich, R. & Marten, I. Malate-induced feedback regulation of plasma membrane anion channels could provide a CO_2 sensor to guard cells. *EMBO J.* **12,** 897-901 (1993).

5. Hedrich, R. *et al*. Malate-sensitive anion channels enable guard cells to sense changes in the ambient CO_2 concentration. *Plant J.* **6,** 741-748 (1994).

6. Holland, I.B., Cole, S.P.C., Kuchler, K. & Higgins, C.F. *ABC Proteins: From Bacteria to Man.* (Academic Press, Amsterdam, 2003).

7. Martinoia, E. *et al.* Multifunctionality of plant ABC transporters – more than just detoxifiers. *Planta* **214,** 345-355 (2002).

8. Rea, P.A. Plant ATP -binding cassette transporters. *Annu. Rev. Plant Biol.* **58,** 347-375 (2007).

9. Verrier, P.J. *et al*. Plant ABC proteins - a unified nomenclature and updated inventory. *Trends Plant Sci.* **13,** 151-159 (2008).

10. Gaedeke, N. *et al*. The *Arabidopsis thaliana* ABC transporter AtMRP5 controls root development and stomata movement. *EMBO J.* **20,** 1875-1887 (2001).

11. Klein, M. *et al*. The multidrug resistance ABC transporter AtMRP5 is involved in guard cell hormonal signaling and drought tolerance. *Plant J.* **33,** 119-129 (2003).

12. Suh, S. *et al*. The ATP-binding cassette transporter AtMRP5 modulates anion and Ca^{2+} channel activities in *Arabidopsis* guard cells. *J. Biol. Chem.* **282,** 1916-1924 (2007).

13. Dewitt, N.D, Hong, B., Sussman, M.R. & Harper, J.F. Targeting of two *Arabidopsis* H^{+}-ATPase isoforms to the plasma membrane. *Plant Physiol.* **112,** 833-844 (1996).

14. Kobae, Y. *et al*. Loss of AtPDR8, a plasma membrane ABC transporter of *Arabidopsis thaliana* causes hypersensitive cell death upon pathogen infection. *Plant Cell Physiol.* **47,** 309-318 (2006).

15. Schroeder, J.I., Allen, G.J., Hugouvieux, V., Kwak J.M. & Waner, D. Guard cell signal transduction. *Annu. Rev. Plant Physiol. Plant Mol. Biol.* **52,** 627-658 (2001).

16. Schroeder J.I., Kwak J.M. & Allen G.J. Guard cell abscisic acid signal transduction network and engineering of plant drought hardiness. *Nature* **410,** 327-330 (2001).

17. MacRobbie, E.A.C. Signal transduction and ion channels in guard cells. *Phil. Trans. Roy. Soc. London.* **1374,** 1475-1488 (1998).

18. Vavasseur, A. & Raghavendra, A.S. Guard cell metabolism and CO_2 sensing. *New Phytol.* **165,** 665-682 (2005).

19. Young, J.J. *et al*. CO_2 signaling in guard cells: calcium sensitivity response modulation, a Ca^{2+}-independent phase, and CO_2 insensitivity of the *gca2* mutant. *Proc. Natl. Acad. Sci.* **103,** 7506-7511 (2006).

20. Hashimoto, M. *et al*. *Arabidopsis* HT1 kinase controls stomatal movements in response to CO_2. *Nature Cell Biol*. **8,** 391-397 (2006).

21. Hedrich, R. *et al*. Changes in apoplastic pH and membrane potential in leaves in relation to stomatal responses to CO_2, malate, abscisic acid or interruption of water supply. *Planta* **213,** 594-601 (2001).

22. Raschke, K. Alternation of the slow with the quick anion conductance in whole guard cells effected by external malate. *Planta* **217,** 651-657 (2003).

23. Schroeder J.I. Anion channels as central mechanisms for signal transduction in guard cells and putative functions in roots for plant-soil interactions. *Plant Mol. Biol.* **28,** 353-361 (1995).

24. Keller, B.U., Hedrich, R., & Raschke, K. Voltage-dependent anion channels in the plasma membrane of guard cells. *Nature* **341,** 450-453 (1989).

25. Negi, J. *et al.* CO_2 regulator SLAC1 and its homologues are essential for anion homeostasis in plant cells. *Nature* **452,** 483-486 (2008).

26. Vahisalu, T. *et al*. SLAC1 is required for plant guard cell S-type anion channel function in stomatal signaling. *Nature* **452,** 487-491 (2008).

27. Geisler, M. *et al*. Cellular efflux of auxin catalyzed by the *Arabidopsis* MDR/PGP transporter AtPGP1. *Plant J.* **44,** 179-194 (2005).

28. Hunke, S., Döse, S., & Schneider, E. Vanadate and bafilomycin A1 are potent inhibitors of the ATPase activity of the reconstituted bacterial ATP-binding cassette transporter for maltose (MalFGK2). *Biochem Biophys Res Commun*. **216,** 589-594 (1995)

29. Hurth, M.A. *et al*. Impaired pH homeostasis in *Arabidopsis* lacking the vacuolar dicarboxylate transporter and analysis of carboxylic acid transport across the tonoplast. *Plant Physiol*. **137,** 901-910 (2005).

30. Van Kirk, C.A. & Raschke, K. Release of malate from epidermal strips during stomatal closure. *Plant Physiol.* **61,** 474-475 (1978).

31. Abel, S. & Theologis, A. Transient gene expression in protoplast of *Arabidopsis thaliana*. *Methods Mol. Biol.* **82,** 209-217 (1998).

32. Hwang, J.U. *et al*. Actin filaments modulate both stomatal opening and inward K^+-channel activities in guard cells of *Vicia faba* L. *Plant Physiol.* **115**, 335-342 (1997).

33. Endler, A. *et al*. Identification of a vacuolar sucrose transporter in *Hordeum vulgare* and *Arabidopsis thaliana* by a tonoplast proteomic approach. *Plant Physiol.* **141,** 196-207 (2006).

34. Jeong, J. *et al*. A nodule-specific dicarboxylate transporter from alder is a member of the peptide transporter family. *Plant Physiol.* **134,** 969-978 (2004).

35. Kimoto, E. *et al*. Efflux transport of N-monodesethylamiodarone by the human intestinal cell-line Caco-2 cells. *Drug Metab. Pharmacokinet.* **22,** 307-312 (2007).

Supplementary Information is linked to the online version of the paper at www.nature.com/nature. A figure summarizing the main result of this paper is included as Supplementary Information, Fig. S1.

Acknowledgement We thank Prof. N. Amrhein, Swiss Federal School of Technology for reading the manuscript and Dr. A. Vavasseur for helpful discussion on gas exchange measurements and M. Schellenberg for making section image of AtABCB14:GUS. This project was supported by Global Research Laboratory program of Ministry of Science and Technology of Korea. The work in the laboratory of E.M. was partially supported by the Swiss National Foundation.

Author contributions M.L. performed most of the experiments. Y.C. and J.-Y.Y. supported the HeLa cell experiments. B.B. contributed to the gas exchange experiment. Y.-Y.K. and M.M. contributed to the membrane fractionation experiment. B.J. contributed to the localization study. E.M. and Y.L. designed the experiments and wrote the manuscript.

Author Information The authors declare no competing financial interests.

Correspondence and requests for materials should be addressed to Y.L. (ylee@postech.ac.kr).

Figure 1 AtABCB14 is mainly expressed in guard cells and localizes at the plasma membrane. (**a-f**) *AtABCB14* promoter-GUS (*pAtABCB14*::GUS) reporter gene expression of five week-old plants. (**a**) leaf (**b**) leaf close-up (**c**) leaf cross-section (**d**) flower (**e)** stem (**f**) silique. Scale bars represent 0.5 cm, 15 μm, 100 μm, 0.5 cm in **a**, **b**, **c**, and **d**-**f**, respectively. (**g**) RT-PCR analysis of *AtABCB14* expression in guard cells (GC) and mesophyll cells (MC). *AtABCB14* transcript level was 1.44 folds higher in guard cells than in mesophyll cells when normalized to the intensity of the loading control *EF-1α* band. (**h-l**) Subcellular localization of the AtABCB14:GFP fusion protein transiently expressed in mesophyll protoplasts. Bright-field (**h**) and fluorescence (**i**) images of two *AtABCB14:GFP*-transformed (top and bottom) and one non-transformed (center) cell. (**j-l**) Colocalization of AtABCB14:GFP with the plasma-membrane marker AtAHA2:RFP. Scale bars represent 10 μm. (**m**) Intracellular localization of AtABCB14:HA detected by fractionation of microsomes on a sucrose density gradient. Fractions were collected and immunoblotted with antibodies to HA, as well as to plasma membrane (AtPDR8), ER (Bip) and vacuolar membrane (γ-TIP) markers. (**n**) Plasma membrane localization of AtABCB14:sGFP in guard cells of *Arabidopsis* plants expressing AtABCB14:sGFP under the *AtABCB14* native promoter. Full scanned images for **g** and **m** are shown in Supplementary Information, Fig. S6. Scale bar represents 5 μm.

Figure 2 AtABCB14 affects stomatal closure in response to elevated [CO_2] and malate. (**a**) Stomatal apertures of detached whole leaves under high [CO_2]. Leaves were floated on 10 mM KCl buffer for 3 hours (Initial), and then incubated for 0.5 h with 700 ppm CO_2 (CO_2). Data represent means ± s.e.m. of 150 stomata (measured in three independent experiments). (**b**) Time course of stomatal conductance change in response to elevated [CO_2]. Stomatal conductance of wild type, *atabcb14-1* and *2* was measured using gas exchange

system. The leaves were stabilized in 100 ppm CO_2 before changing to 800 ppm CO_2. Values of stomatal conductance at 100 ppm CO_2 were normalized to 1. Seven rosette leaves were used in each set. Error bars represent s.e.m. Initial rates in decrease of stomatal conductance after raising [CO_2] from 100 to 800 ppm were 0.067 and 0.062 relative conductance units per minute for the mutants *atabcb14-1* and *2*, respectively, and 0.040 for wild-type plants. (**c**) Stomatal movement under malate-treated condition. Irradiated leaves in 10 mM KCl buffer were transferred into the 20 mM malate buffer (MA) and incubated for 30 minutes. Data represent means ± s.e.m. of 150 stomata (measured in three independent experiments). (**d**) Effects of CO_2 and malate on stomatal closing of epidermal strips. Epidermal strips, peeled from leaves that were previously illuminated for 2.5 h, were incubated on 10 mM KCl buffer for 1 h (initial apertures), and then treated with 1,000 ppm CO_2 (CO_2) or 20 mM malate buffer (MA) for 0.5 h under white light (200 µmol m^{-2} s^{-1}). Measured stomata had no viable neighbour cells (tested by FDA staining[19]). Data are means ± s.e.m of n=120 (obtained from four independent experiments). (**e**) Light-induced stomatal opening of detached leaves on malate buffer. Detached whole leaves were incubated on 5 mM malate buffer for the times indicated. Data represent means ± s.e.m. (n=180 stomata per time point, obtained from three experiments). * $p < 0.05$; comparison to wild type in the same treatment, $^{\blacktriangle}p < 0.05$; comparison to initial value of the same genotype (Student's *t* test).

Figure 3 AtABCB14 mediates malate transport. (**a**) Functional complementation of the *E. coli* dicarboxylate transport mutant strain by heterologous expression of *Arabidopsis* AtABCB14. Mutant strain (CBT315) and its isogenic wild type (K12) were transformed with the vector harbouring the *AtABCB14* gene under the control of the *tac* promoter (A14) or with the empty vector (EV). Strains were grown for four days at 37°C on M9 agar medium with 10 mM L-malic acid as the

sole carbon source. (**b**) Time dependence of ^{14}C-malic acid uptake by the CBT315 mutant strain transformed with the same *AtABCB14* vector (A14) or empty vector (EV) as in (**a**) at 1 mM malate and pH=5.9. Data represent means ± s.e.m. (n=8, from two separate experiments). (**c**) Inhibitors of ABC transporters reduce AtABCB14-dependent ^{14}C-malate uptake of CBT315 cells expressing AtABCB14. Cells were pre-incubated with vanadate (VD), verapamil (VP), or cyclosporin A (CsA) and as control without inhibitor (A14) for 20 minutes. Malate uptake was measured after 15 min incubation in 1 mM malate (pH=5.9) as described in (**b**). To calculate AtABCB14-specific malate uptake, activities were subtracted with uptake activities of the empty vector control incubated with the corresponding inhibitor at the same conditions. Data represent means ± s.e.m. (n=12, from three experiments). (**d**) Effect of various organic and inorganic anions on the AtABCB14-dependent ^{14}C-malate uptake of CBT315 cells expressing AtABCB14. Uptake was measured at 0.5 mM malate (pH=5.9) with or without the presence of additional 1.5 mM of the respective anion. Data represent means ± s.e.m. (n=12, from three experiments). (**e**) ^{14}C-malic acid uptake in HeLa cells transformed with the empty vector (left bar) or a vector containing *AtABCB14* (right bar). Incubation was for 10 min and the 0 min value (59.9±4.0 dpm and 57.5±2.8 dpm for empty vector control and AtABCB14 expressing cells, respectively) was subtracted. The inset shows the presence of *AtABCB14* transcript in cells transfected with *AtABCB14.* Full scanned image is shown in Supplementary Information, Fig. S6. Data represent mean ± s.e.m. (n=9, from 3 experiments). *p < 0.05; comparison to EV at each time points (**b**), A14 (**c**), control (**d**) and empty vector (**e**), respectively, by Student's *t* test.

Figure 4 *AtABCB14* mutants display different flowering times. (**a, b**) 8 week-old wild-type, *AtABCB14 k*nockout (*atabcb14-1*) and overexpressing (*35S:A14-1*)

plants grown under standard (**a**) and under combined high [CO_2] and drought conditions (**b**). (**c, d**) From these genotypes also flowering times (**c**) and total rosette leaf numbers at time of flowering (**d**) under standard and combined high [CO_2] and drought growth conditions was determined. Seeds of wild type, *atabcb14-1*, and *35S::A14-1* were sown on soil, and grown for 2 weeks under the conditions described in Methods. Subsequently, plants were divided into two groups: the first group was kept under control conditions while the second group was transferred into a high [CO_2] (700 ppm) growth chamber. All plants were grown for additional 6 weeks (**a, b**) or until flowering occurred (**c, d**). The plants in the high [CO_2] chamber were watered only once 14 days after the transfer. Flowering time and leaf numbers are means ± s.e.m. (n=22, from three experiments, *$p < 0.05$; comparison to *atabcb14*-1 in the same treatment, ▲$p<0.05$; comparison to wild type in the same treatment, by Student's *t* test). Bars represent 5 cm.

Fig. 1

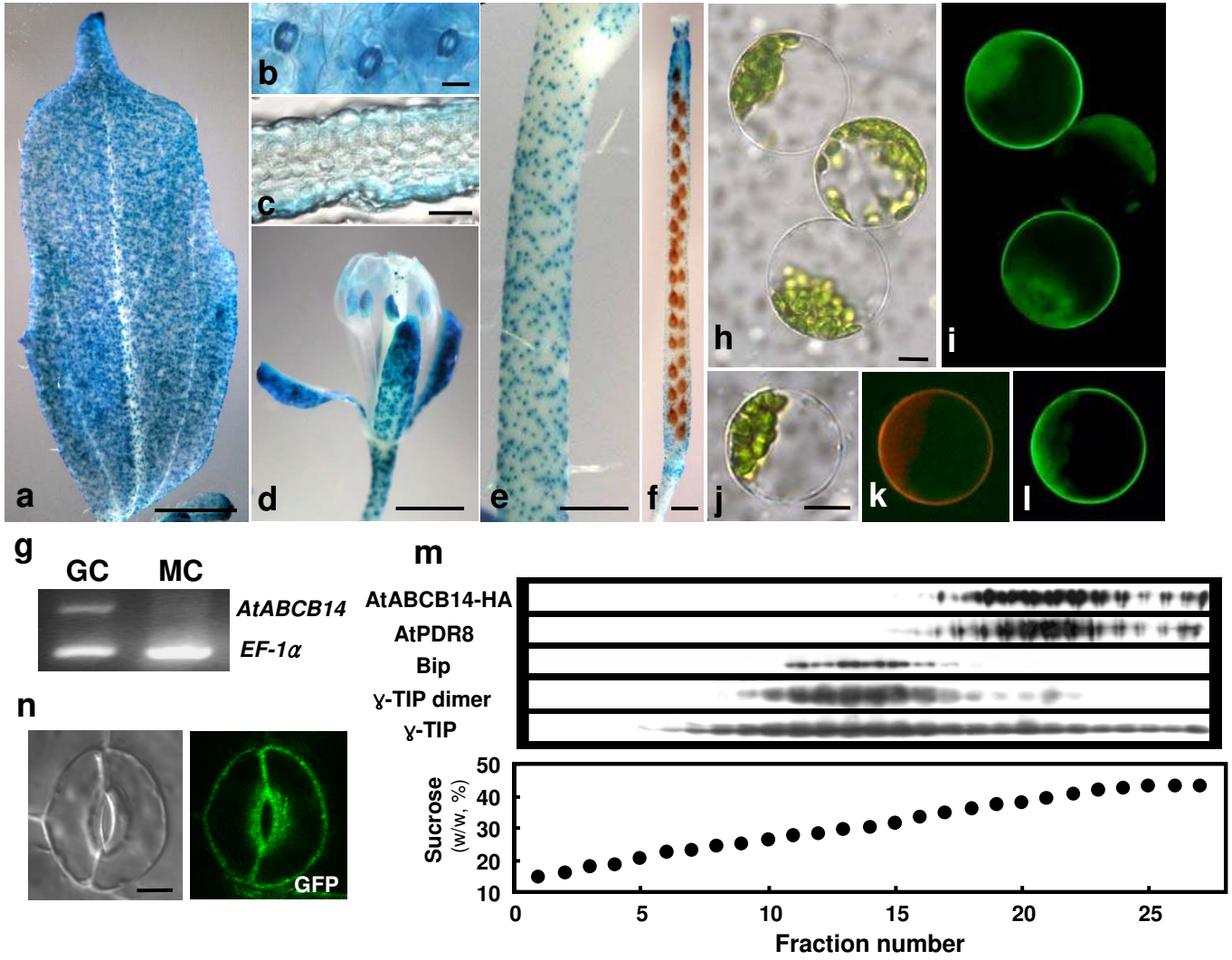
a
b
c
d
e
f
h
i
j
k
l
g
GC
MC
AtABCB14
EF-1α
n
GFP
m
AtABCB14-HA
AtPDR8
Bip
γ-TIP dimer
γ-TIP
Sucrose (w/w, %)
50
40
30
20
10
0
5
10
15
20
25
Fraction number

Fig. 2

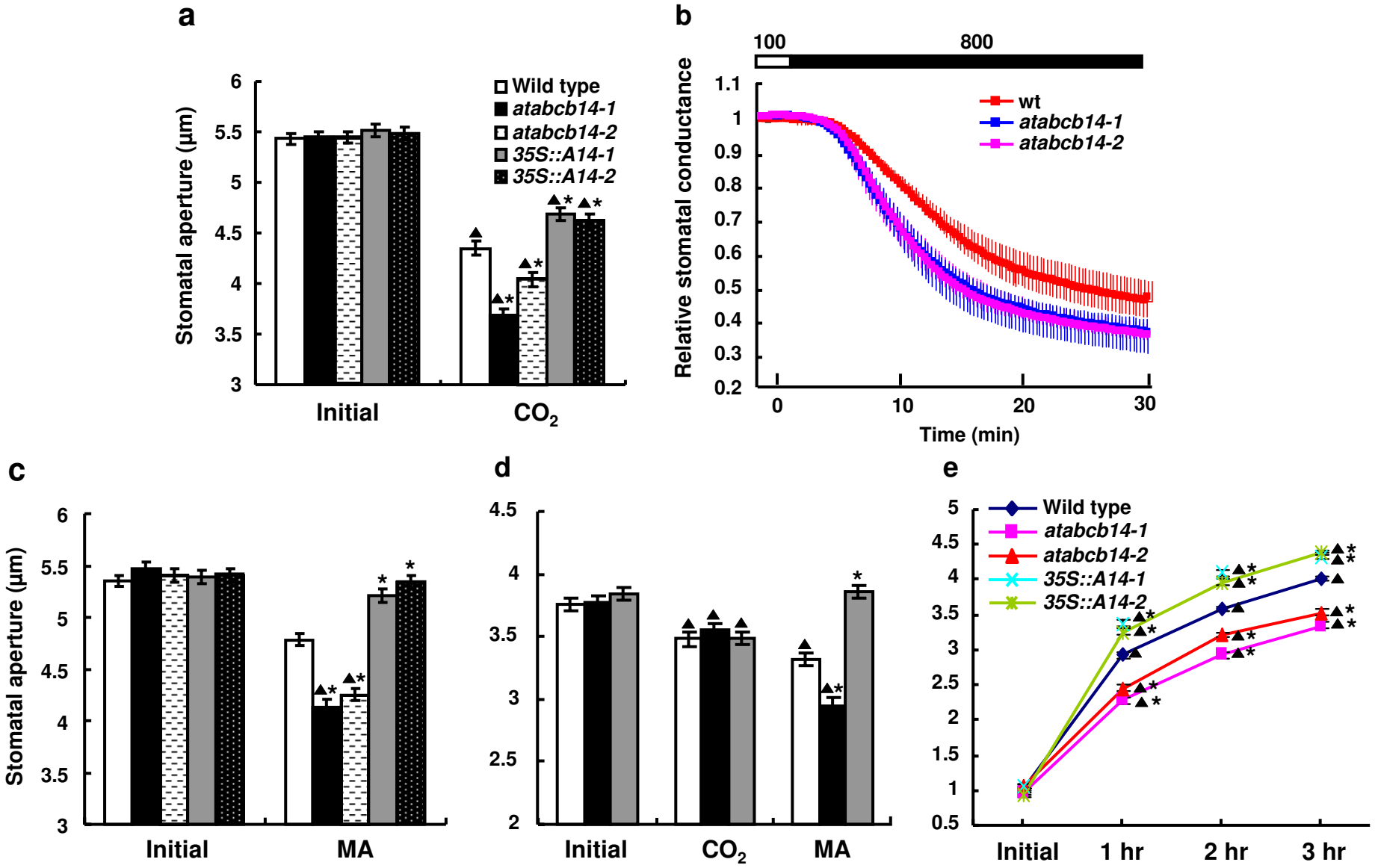
a
Stomatal aperture (μm)
Wild type
atabcb14-1
atabcb14-2
35S::A14-1
35S::A14-2
Initial
CO2
b
100
800
Relative stomatal conductance
wt
atabcb14-1
atabcb14-2
Time (min)
c
Stomatal aperture (μm)
Initial
MA
d
Initial
CO2
MA
e
Wild type
atabcb14-1
atabcb14-2
35S::A14-1
35S::A14-2
Initial
1 hr
2 hr
3 hr

Fig. 3

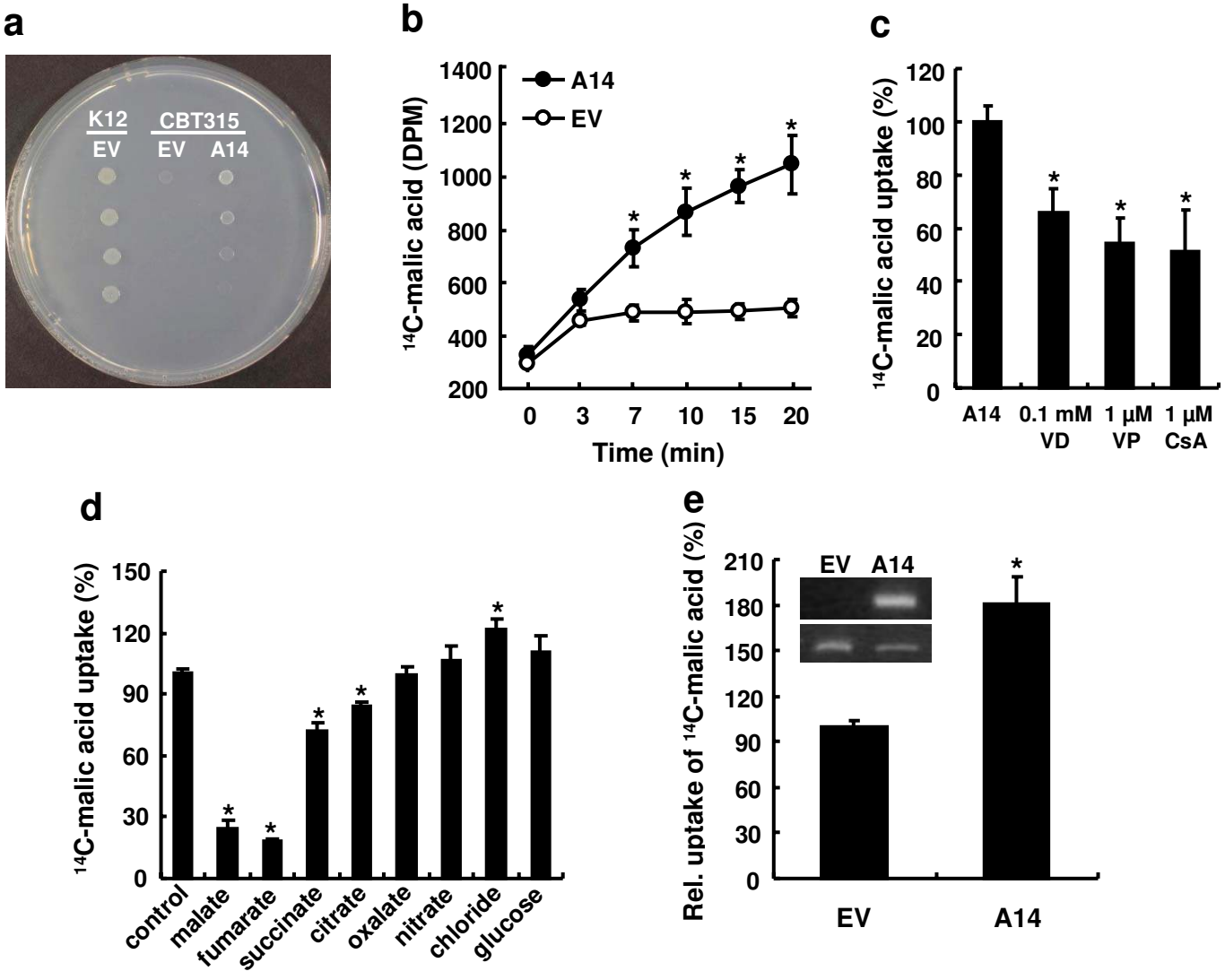
a
K12
CBT315
EV
EV
A14
b
A14
EV
^{14}C-malic acid (DPM)
1400
1200
1000
800
600
400
200
0
3
7
10
15
20
Time (min)
c
^{14}C-malic acid uptake (%)
120
100
80
60
40
20
0
A14
0.1 mM VD
1 µM VP
1 µM CsA
d
^{14}C-malic acid uptake (%)
150
120
90
60
30
0
control
malate
fumarate
succinate
citrate
oxalate
nitrate
chloride
glucose
e
Rel. uptake of ^{14}C-malic acid (%)
210
180
150
120
90
60
30
0
EV
A14
EV
A14

Fig. 4

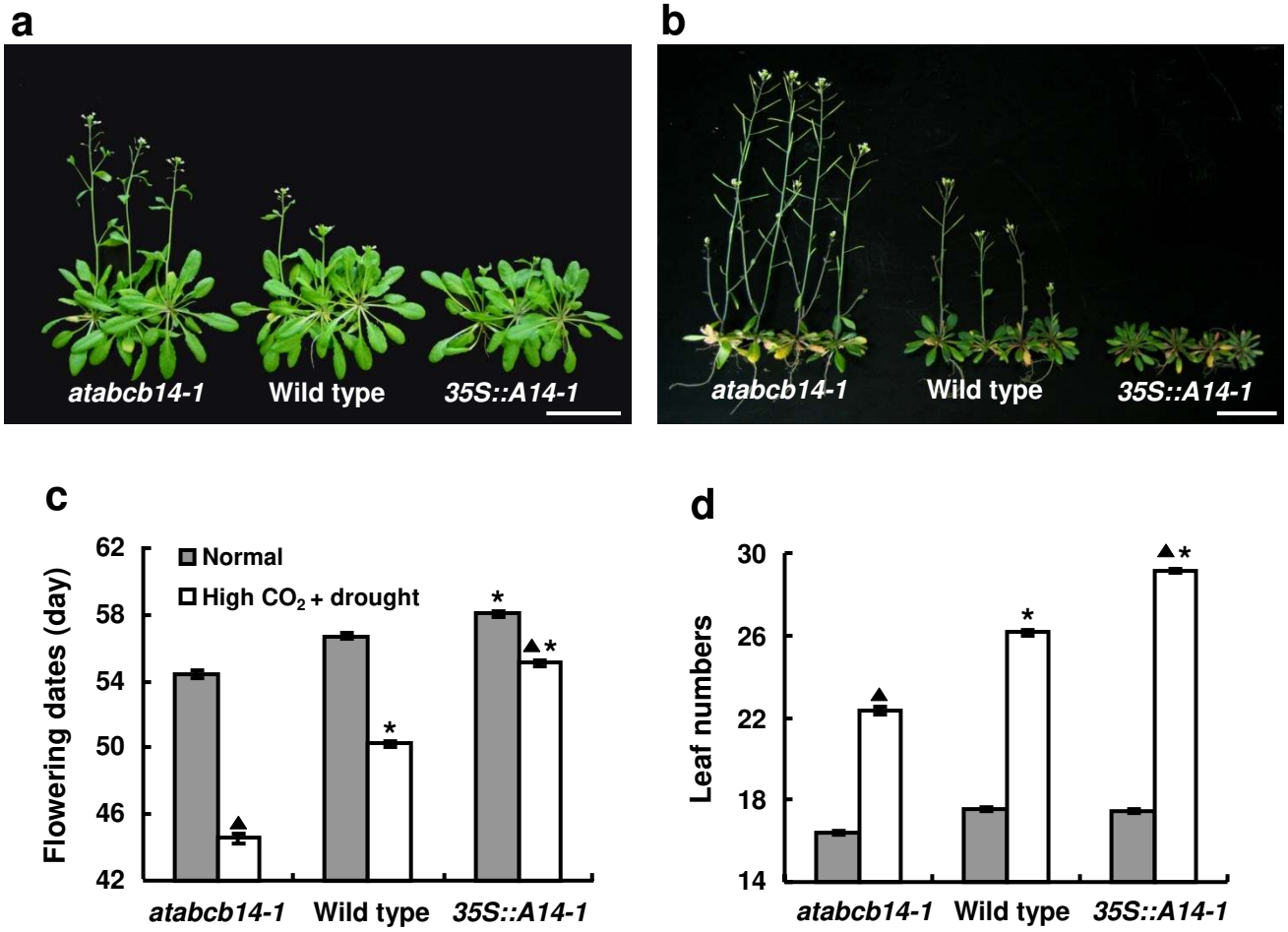
a
b
atabcb14-1
Wild type
35S::A14-1
atabcb14-1
Wild type
35S::A14-1
c
Flowering dates (day)
62
58
54
50
46
42
Normal
High CO2 + drought
*
▲*
▲
*
atabcb14-1
Wild type
35S::A14-1
d
Leaf numbers
30
26
22
18
14
▲*
*
▲
atabcb14-1
Wild type
35S::A14-1

SUPPLEMENTARY INFORMATION

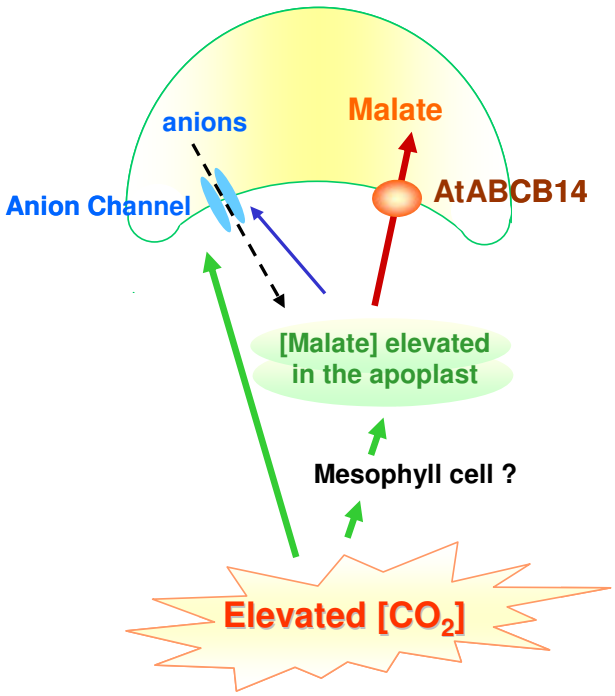

Figure S1 The role of AtABCB14 in stomatal response to elevated [CO_2]. Elevated [CO_2] activates anion channels at the plasma membrane of guard cells, releasing malate into apoplast. Mesophyll cells may also play a role in increasing the concentration of malate in the apoplast. Malate at the apoplast of guard cells also activates the anion channels, resulting in additional malate efflux and stomatal closing. AtABCB14 takes up malate into guard cells, where the organic acid acts as an osmoticum, thereby reducing the speed of the stomatal closing movement.

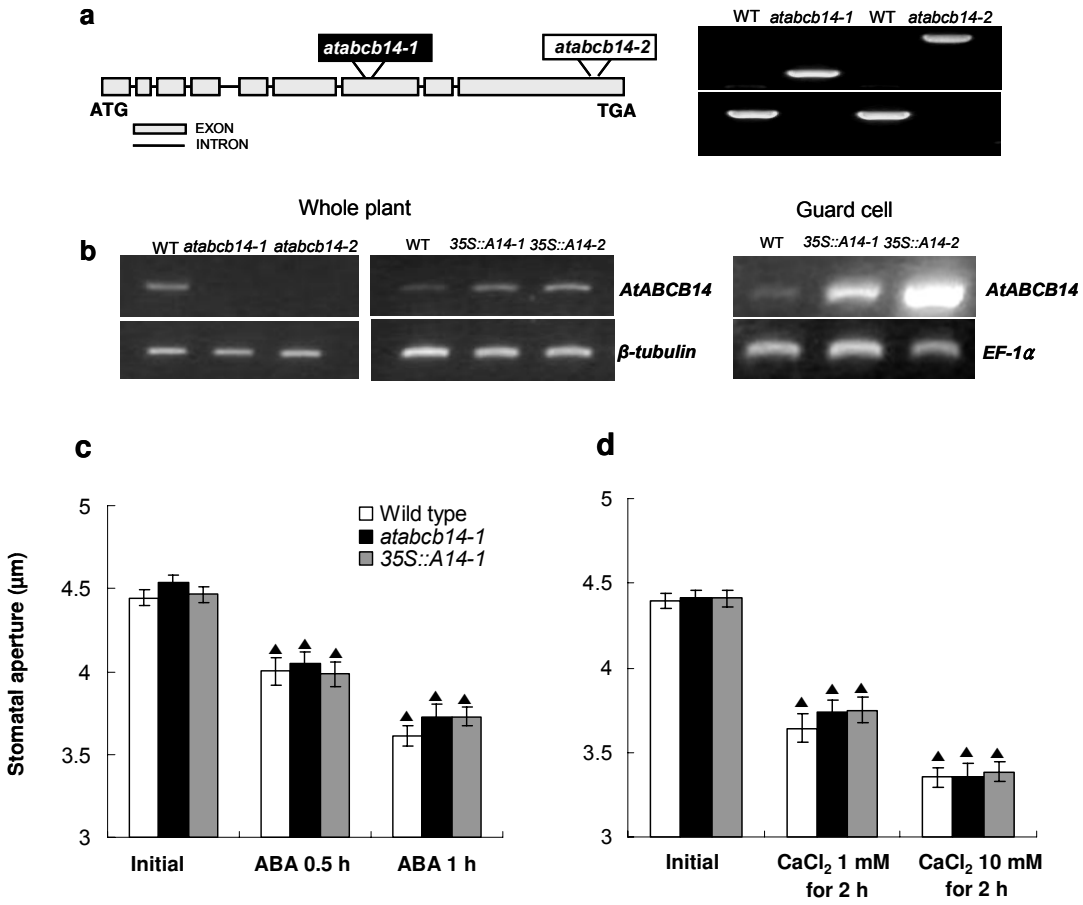

Figure S2 Selection of AtABCB14 transgenic *Arabidopsis* and stomatal movement under ABA or calcium treated condition. (**a**, **b**) Selection of AtABCB14 knockout and over-expressing *Arabidopsis* (**a**) T-DNA insertion sites in the *AtABCB14* gene of the two alleles of the knockout. Gel image in the right shows genotype determination by PCR of two alleles of AtABCB14 knockout plants. Upper and lower images show T-DNA specific, and *AtABCB14* specific bands, respectively. (**b**) *AtABCB14* transcript levels of wild type and AtABCB14 transgenic lines. The transcripts of *AtABCB14* were detected by RT-PCR. Total RNA of wild type (WT), AtABCB14 knockout (*atabcb14-1,2*) and over-expressing lines (*35S::A14-1,2*) were extracted from 14 day-old *Arabidopsis* seedlings (image in left and center) or guard cell protoplast collected by patch pipettes (image in right). *AtABCB14* transcript levels were 1.5 and 1.7 folds higher in *35S::A14-*

1 and *35S::A14-2* plants, respectively, than that of wild type, when normalized to the intensity of the loading control *β-tubulin* band. *AtABCB14* transcript levels were 1.9 and 4.2 folds higher in *35S::A14-1* and *35S::A14-2* guard cell protoplasts, respectively, than that of wild type, when normalized to the intensity of the loading control *EF-1α* band. Full scanned images are shown in Supplementary Information, Fig. S6. (**c**, **d**) ABA or calcium induced stomatal closing. Illuminated leaves were transferred into 10 mM KCl buffer containing 1 μM ABA (**c**) or 1 and 10 mM $CaCl_2$ (**d**) and their stomatal apertures were measured. Averages ± s.e.m. (3 experiments, n=120 for **c**, and 150 for **d**). $^{\triangle}p < 0.05$; comparison to initial values by Student's *t* test. Between different genotypes, there was no statistically significant difference.

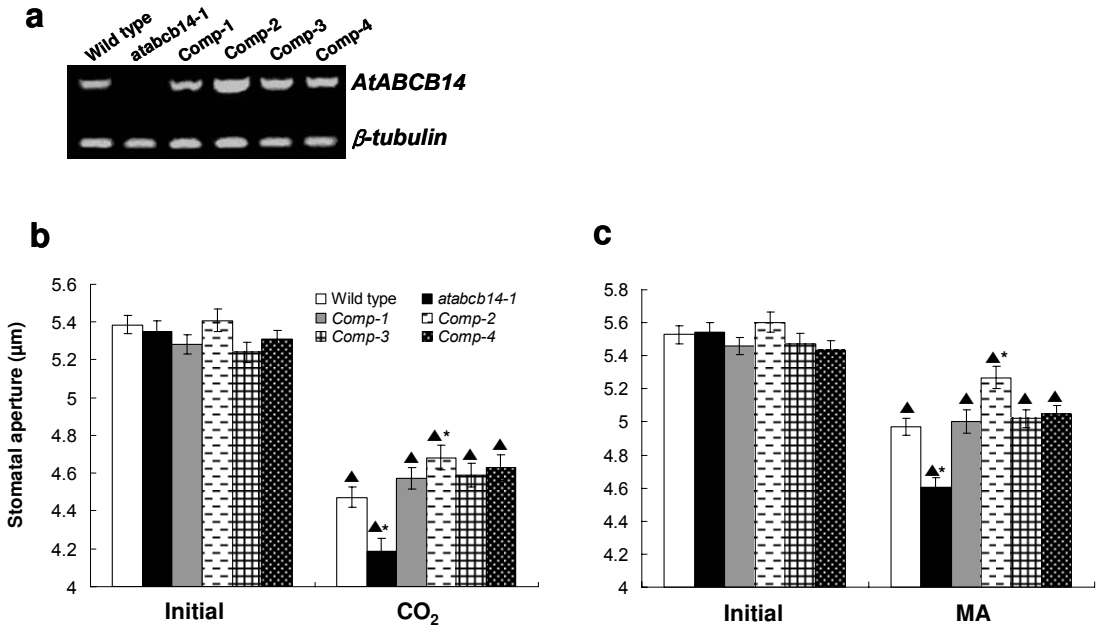

Figure S3 *AtABCB14* expression level and stomatal movement of AtABCB14 complementation lines. (**a**) mRNA expression level of wild type, *atabcb14-1*, and 4 independent complementation lines (*Comp-1, 2, 3, 4*) assayed by RT-PCR. RT-PCR was performed using total RNA extracted from 2 week-old seedlings. *β-tubulin* was used as a loading control. Full scanned image is shown in Supplementary Information, Fig. S6. (**b**, **c**) High $[CO_2]$ (**b**) or malate (**c**) induced stomatal closing. Detached leaves were floated on 10 mM KCl-MES buffer and irradiated with white light for 3 hours (initial), and then transferred to 700 ppm $[CO_2]$ (**b**) or 20 mM malate (**c**) and incubated for additional 0.5 h. Averages ± s.e.m. (3 experiments, n=150). $^{\triangle}p<0.05$; comparison to the initial values, $^{*}p<0.05$; comparison to wild type value in the same condition. *P* values are calculated by Student's *t* test.

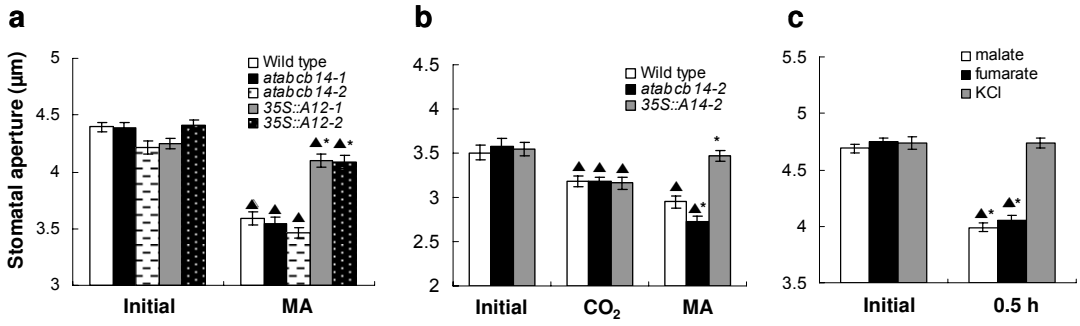

Figure S4 Stomatal movement under high [CO_2], malate, or fumarate treated condition. (a) Stomatal closing induced by 5 mM malate in whole leaves. Detached leaves were floated on 10 mM KCl-MES and irradiated with white light for 3 hours (initial), and then transferred to 5 mM malate buffer (MA) and incubated for additional 0.5 h (**b**) Stomatal apertures in epidermal strips treated with high $[CO_2]$ or malate. Experimental procedures were the same as described for Fig. 2d. (**c**) Fumarate induces stomatal closure similarly as malate. Detached leaves were illuminated for 3 hours to induce stomatal opening and then transferred into 20 mM malic acid (malate), 20 mM fumaric acid (fumarate), or 10 mM KCl buffer as described in Methods. Averages ± s.e.m. (3 experiments, n=150 for **a** and **b**, n=120 for **c**). $^{\triangle}p<0.05$; comparison to the initial values, $^{*}p<0.05$; comparison to wild type value in the same condition. *P* values are calculated by Student's *t* test.

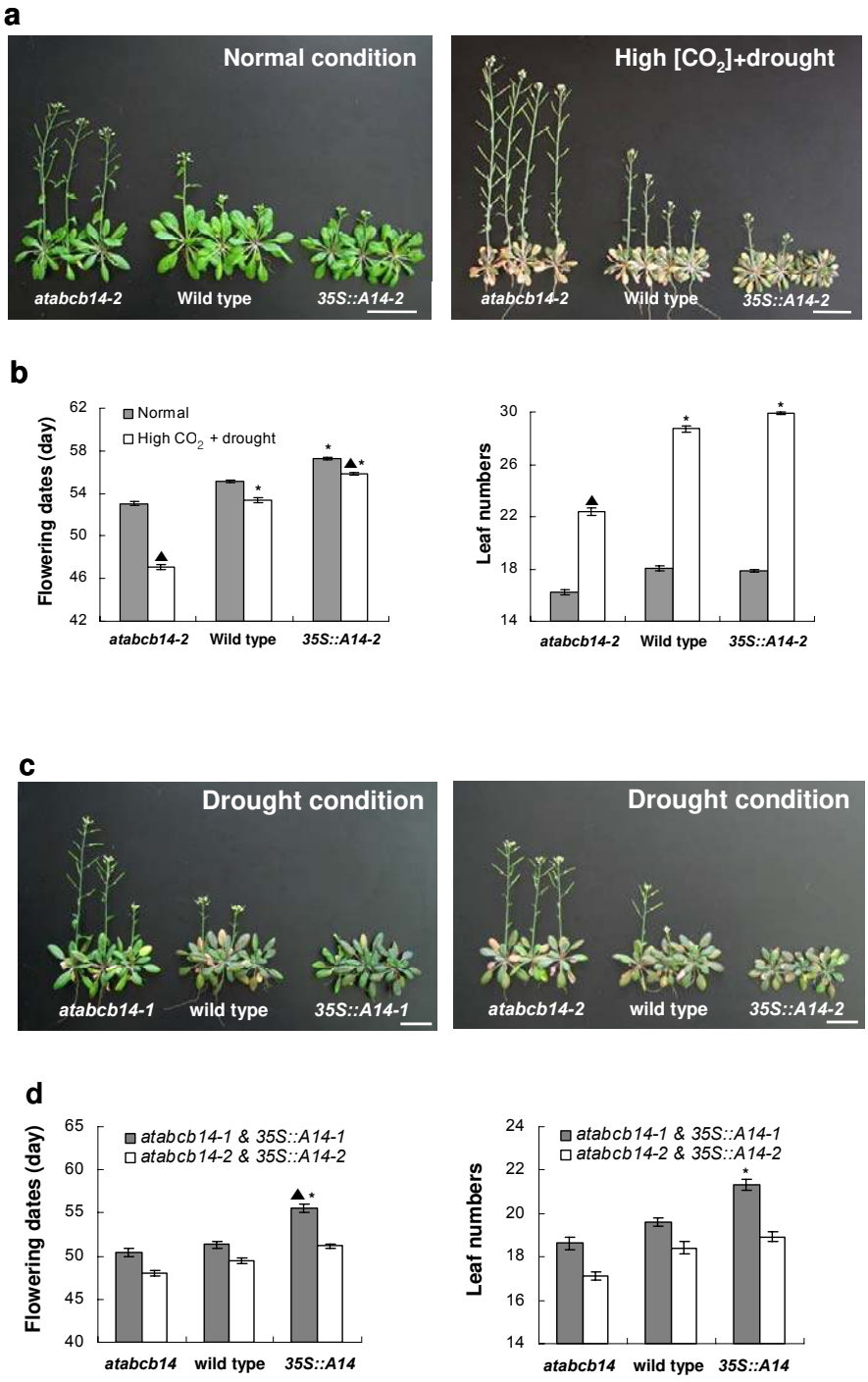

Figure S5 Flowering times of *AtABCB14* mutant plants. (**a**, **b**) Flowering time of additional lines of AtABCB14 transgenic plants under control or high [CO_2] and drought condition. (**a**) Growth under control and high [CO_2] and drought condition. Growth condition of AtABCB14 transgenic plants was the same as the method described in

Figure 4. (**b**) Flowering time and leaf numbers of AtABCB14 transgenic plants. (**c**, **d**) Flowering times of *AtABCB14* mutant plants under drought condition. (**c**) Growth of AtABCB14 transgenic plants under drought condition. Seeds of wild type, and AtABCB14 transgenic plants were sown on soil, and grown for 4 weeks under the conditions described in Methods. Subsequently, plants were exposed to drought condition for 33 day. (**d**) Flowering time and leaf numbers of AtABCB14 transgenic plants. Flowering dates and leaf numbers are averages ± s.e.m. (3 experiments for **b**, 17<n<23, 2 experiments for **c**, 12<n<15). Bars represent 5 cm. *$p < 0.05$; comparison to *atabcb14-1 or 2* and $^{\triangle}p<0.05$; comparison to wild type by Student's *t* test.

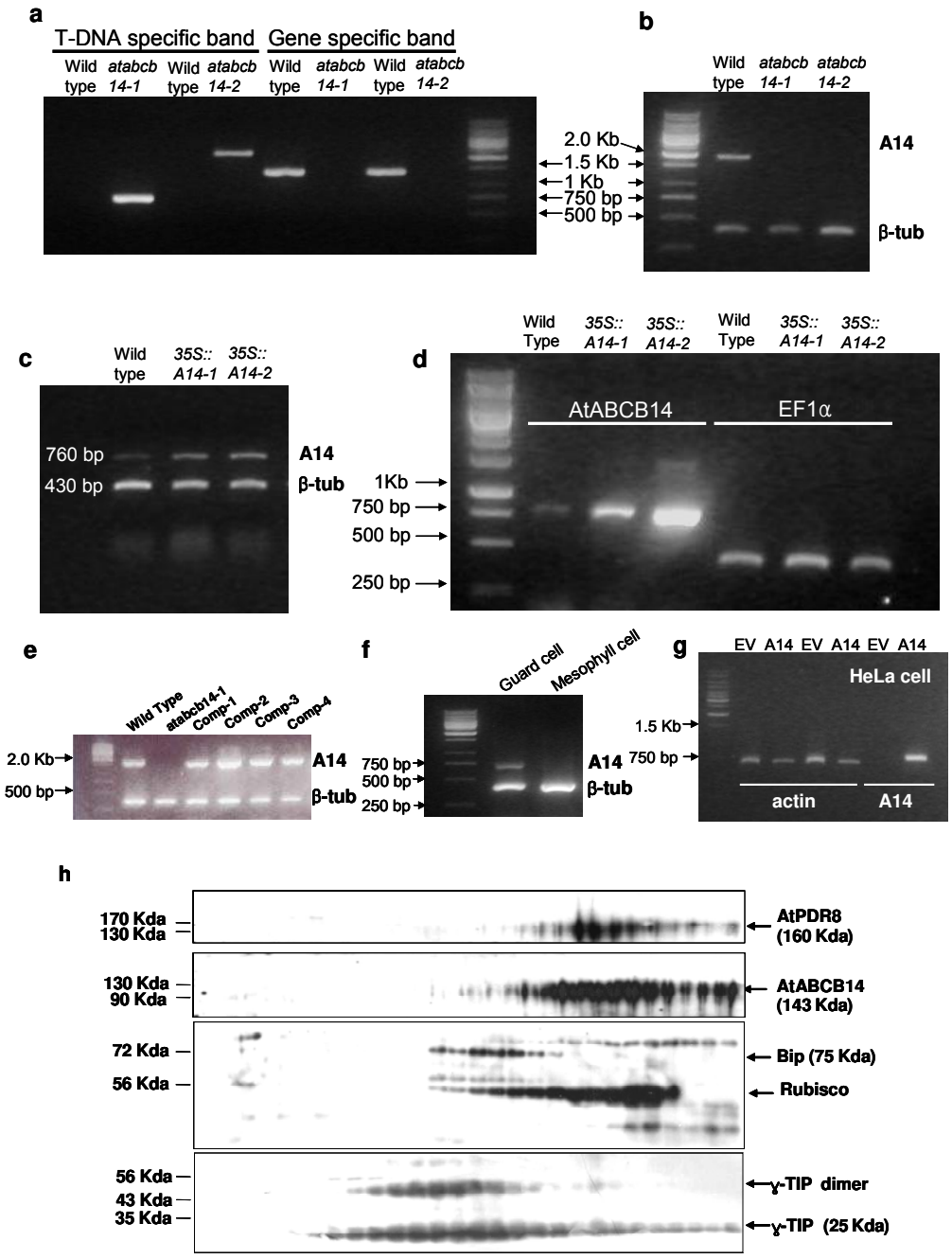

Figure S6 Full scanned images of (**a**) Genotyping reaction (Figure S2a) (**b**-**g**) RT-PCR reaction (**b**-**d** for Figure S2b, **e** for Figure S3a, **f** for Figure 1g, and **g** for Figure 3e) (**h**) Western blot with anti-AtPDR8 (first column), anti-HA (second column), anti-Bip (third column), and anti-γ-tip (fourth column).